Electronic Supplementary Information (ESI) for

Trapping a Pentagonal Molecule in a Self-Assembled Molecular Network: an Alkoxylated Isosceles Triangular Molecule Does the Job

Masaru Anzai,[†] *Iyoda Masahiko,*[|] *Steven De Feyter,*[‡] *Yoshito Tobe,*[¶,#] *Kazukuni Tahara*[*,†]

[†]Department of Applied Chemistry, School of Science and Technology, Meiji University, 1-1-1 Higashimita, Tama-ku, Kawasaki, Kanagawa, 214-8571, Japan, [|]Graduate School of Science, Tokyo Metropolitan University, 1-1 Minami-osawa, Hachioji, Tokyo 192-0397, Japan, [‡]Division of Molecular Imaging and Photonics, Department of Chemistry, KU Leuven, Celestijnenlaan 200 F, 3001 Leuven, Belgium, [#]The Institute of Scientific and Industrial Research, Osaka University, Ibaraki, Osaka 567-0047, Japan, [¶]Department of Applied Chemistry, National Chiao Tung University, 1001 Ta Hsueh Road, Hsinchu 30030, Taiwan

correspondence to: tahara@meiji.ac.jp

This file includes:

1. Experimental Details

1.1 Synthesis of [14]ISODBA

Scheme S1. Synthesis of **[14]ISODBA**.

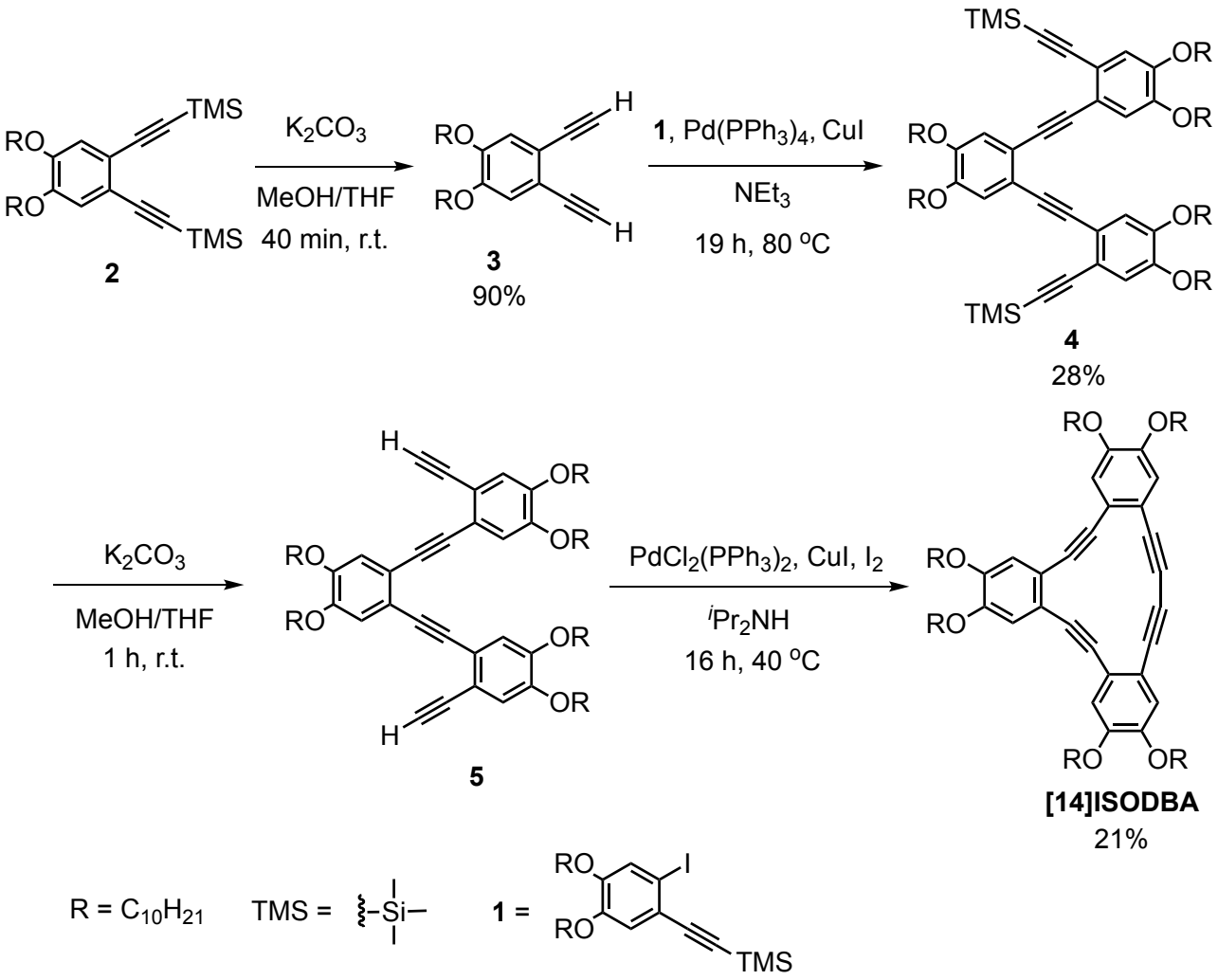

General. The solvents, NEt_3, MeOH and $^iPr_2NH$ were distilled before use. DMF was distilled from CaH_2. THF was purified by passed through activated alumina and copper catalyst in a Glass Contour solvent purification system prior use. $PdCl_2(PPh_3)_2$ and $Pd(PPh_3)_4$ were prepared following the literatures.[1,2] All other commercially available reagents were used as received.

^1H (500 MHz) and ^{13}C (125 MHz) NMR spectra were measured on a JEOL ECA-500 spectrometer. For all measurements, chloroform-*d* was used as the solvent, and the spectra were referenced to

tetramethylsilane signals in the ^{1}H and ^{13}C NMR spectra (0.00 ppm), respectively. Silica gel column chromatography was conducted using silica gel 60N (spherical shape and neutral, Kanto Chemical CO., INC.) Preparative HPLC was undertaken with a JAI LC-908 or LaboACE LC-5060 chromatograph using 600 mm × 20 mm JAIGEL-1H and 2H columns with $CHCl_3$ as the eluent. Other spectra were recorded by the use of the following instruments: IR spectra, JACSCO FT/IR-4100; mass spectra, JMS-T100GCV.

Synthesis of 1,2-Didecyloxy-4-iodo-5-[(trimethylsilyl)ethynyl]benzene (1) and 1,2-Didecyloxy-4,5-bis[(trimethylsilyl)ethynyl]benzene (2). Under an argon atmosphere, 1,2-didecyloxy-4,5-diiodobenzene (5.00 g, 7.78 mmol), $Pd(PPh_3)_4$ (222 mg, 192 μmol) and CuI (151 mg, 791 μmol) were added to a two necked flask. NEt_3 (100 mL) bubbled with argon gas for 0.5 h was added to this flask. Then, (trimethylsilyl)acetylene (859 mg, 8.74 mmol) was added via a syringe. After stirring at room temperature for 1 h, the reaction mixture was warmed to 80 °C for 3 h with continuous stirring. The reaction mixture was filtered, and $CHCl_3$ (30 mL) and NH_4Cl aq. (30 mL) were added. The mixture was extracted with $CHCl_3$ (30 mL × 3), washed with brine, and the organic phase was dried over $MgSO_4$. After removal of the solvents under vacuum, the crude product mixture was separated by a silica gel column chromatography (hexane/CH_2Cl_2 = 5/1) to afford **1** as a pale yellow oil (2.42 g, 51%) and **2** (960 mg, 21%) as a red-brown oil. All spectra of **1** and **2** agreed with those in previous reports.[3,4]

Synthesis of 1,2-Didecyloxy-4,5-diethynylbenzene (3). Compound **2** (1.59 g, 2.73 mmol) and K_2CO_3 (2.08 g, 1.51 mmol) were added to a round bottom flask. A mixture of MeOH (50 mL) and THF (50 mL) was added to this flask. After stirring at room temperature for 40 min, the mixture was filtered, and ether (30 mL) was added to the filtrate. The products were washed with NH_4Cl aq. (30 mL × 3). The organic phase was dried over $MgSO_4$, and the solvents were removed under vacuum to afford **3** (1.07 g, 90%) as yellow solid. All spectra of **3** agreed with those in a previous report.[4]

Synthesis of Compound 4. Under an argon atmosphere, compound **3** (35.3 mg, 80.4 μmol), $Pd(PPh_3)_4$ (4.34 mg, 3.76 μmol) and CuI (1.11 mg, 5.83 μmol) were added to a two necked flask. A solution of **1** (129 mg, 210 μmol) in NEt_3 (5 mL) was added to this flask via a syringe. After stirring at 80 °C for 19 h, the reaction mixture was filtered, and $CHCl_3$ (30 mL) and NH_4Cl aq. (30 mL) were added to the filtrate. The products were extracted with $CHCl_3$ (30 mL × 3). The organic phase was washed with brine and dried over $MgSO_4$. After evaporation of the solvents, the crude product mixture was separated by a silica gel column chromatography (hexane/CH_2Cl_2 = 10/3) followed by preparative HPLC to afford **4** (23.8 mg, 21%) as pale yellow solid. mp 48.7–50.0 °C; ^{1}H NMR (500 MHz, $CDCl_3$, 23.5 °C) δ 7.00 (s, 2H), 6.98 (s, 2H), 6.90 (s, 2H), 3.99 (t, *J* = 7.0 Hz, 4H), 3.96 (t, *J* = 7.0 Hz, 4H), 3.77 (t, *J* = 7.0 Hz, 4H), 1.87–1.77 (m, 8H), 1.74–1.66 (m, 4H), 1.50–1.20 (m, 84H), 0.93–0.83 (m, 18H), 0.21 (s, 18H); ^{13}C NMR (126 MHz, $CDCl_3$, 25 °C) δ 149.3, 148.9, 148.7, 119.8, 119.2, 117.7, 116.1, 115.9, 115.5, 104.1, 96.6, 91.1, 91.0, 69.2, 69.1, 68.9, 32.0, 31.9, 29.7, 29.6, 29.5, 29.41, 29.36, 29.2, 26.0, 22.7, 14.1, 0.1; IR (KBr) 3091, 2955, 2921, 2852, 2146, 1597, 1514, 1470, 1367, 1249, 1229, 1071, 1021, 857, 842, 756 cm^{-1}; HRMS (FD) *m*/*z* calcd for $C_{92}H_{150}O_6Si_2$ (M^+): 1407.0971, Found: 1407.0907.

Synthesis of [14]ISODBA. Compound **4** (58.2 mg, 41.3 μmol) and K_2CO_3 (28.1 mg, 203 μmol) were added to a round bottom flask. Then, a mixture of MeOH (3 mL) and THF (3 mL) was added to this flask. After stirring at room temperature for 1 h, the mixture was filtered and ether (30 mL) was added to the filtrate. The mixture was washed with NH_4Cl aq. (30 mL × 3) and the organic phase was dried over $MgSO_4$. The solvents were removed under vacuum to afford **5** as red-brown solid. Without further purification, to a solution of $PdCl_2(PPh_3)_2$ (1.90 mg, 2.71 μmol), CuI (780 μg, 4.09 μmol) and I_2 (3.39 mg, 13.4 μmol) in ^{i}Pr$_2$NH (2.0 mL) was added a solution of compound **5** in ^{i}Pr$_2$NH (2.0 mL) dropwise over a period of 10 h using a syringe pump at 40 °C. The mixture was stirred at 40 °C for additional 6 h. After removal of the solvents under vacuum, the crude mixture was separated by a

silica gel column chromatography (hexane/CH_2Cl_2 = 1/1) followed by preparative HPLC to afford **[14]ISODBA** (10.9 mg, 21%) as pale brown solid. mp 57.3–58.9 °C; ^{1}H NMR (500 MHz, $CDCl_3$, 19.2 °C) δ 7.35 (s, 2H), 7.33 (s, 2H), 7.06 (s, 2H), 4.14 (t, *J* = 6.5 Hz, 4H), 4.12 (t, *J* = 7.0 Hz, 4H), 4.05 (t, *J* = 7.0 Hz, 4H), 1.93–1.82 (m, 12H), 1.55–1.20 (m, 84H), 0.95–0.85 (m, 18H); ^{13}C NMR (126 MHz, $CDCl_3$, 19.5 °C) δ 149.7, 148.9, 148.8, 122.7, 118.9, 116.6, 116.2, 115.4, 112.5, 92.7, 91.9, 86.2, 79.0, 69.4, 69.3, 69.1, 31.9, 29.63, 29.61, 29.5, 29.43, 29.38, 29.26, 29.19, 29.07, 26.1, 26.03, 26.00, 22.7, 14.1; IR (ATR, diamond probe) 3081, 2922, 2851, 2205, 2170, 1593, 1504, 1469, 1251, 1228, 1204 cm^{-1}; HRMS (FD) *m*/*z* calcd for $C_{86}H_{132}O_6$ (M^+): 1261.0024, Found: 1261.0030.

1.2 Details of STM Observations

All STM experiments were performed at 20–25 °C using a Nanoscope IIID (Digital Instruments Inc.) with an external pulse/function generator (Agilent 33220A) with negative sample bias. STM tips were mechanically cut from Pt/Ir wire (80%/20%, diameter 0.25 mm).

Prior to STM imaging, **[14]ISODBA** and/or guest molecules were dissolved in distilled 1,2,4-trichrolobenzene (TCI or Nacalai tesque) at various solute concentrations, and then a drop of this solution (10 or 15 μL) was applied on a freshly cleaved surface of highly orientated pyrolytic graphite (HOPG, grade ZYB, Material Quartz, Inc.). In some cases, to minimize kinetic effects on the monolayer formation, the STM observations of the monolayers were conducted after annealing treatment at 80 °C for 3 h in a sealed sample drying oven. For the annealing treatment, a larger amount of the sample solution (20 or 40 μL) was added to a liquid cell placed on the substrate to minimize the effect of solvent evaporation. By changing the tunneling parameters during the STM imaging, namely, the bias voltage applied to the substrate and the average tunneling current, it was possible to switch from the visualization of the adsorbate layer to that of the underlying HOPG substrate. This enabled us to correct for drift effects by the use of SPIP software ver. 4.0.6 or 6.0.13 (Image Metrology A/S). The white colored axes shown in the figures indicate the directions of the main symmetry axes

of graphite underneath the molecular layers.

1.3 Details on Molecular Mechanics Simulations

Molecular mechanics simulations were performed with the Materials Studio 2017 R2 (BIOVIA) using the Forcite module with COMPASS force field. Each initial geometry of **[14]ISODBA**, **[12]DBA** and **[5]CMPA** was built from the respective molecular model whose structure was optimized by the density functional theory (B3LYP/6-31G(d)) using Gaussian 16, Revision A.03.[5] Then, the orientation of the alkyl chains relative to the π-system was adjusted according to that observed in the STM images. The molecules were placed 0.35 nm above the first layer of a periodic two-layer sheet of graphite (interlayer distance of graphite is 0.335 nm). The graphite structure was frozen during the simulations, and a cutoff of 2.0 nm was applied for the van der Waals interactions (Lennard-Jones type). All simulations were performed under periodic boundary conditions (PBC) which correspond the experimentally derived unit cell parameters.

2. Molecular Models and Conceived Co-Assemblies

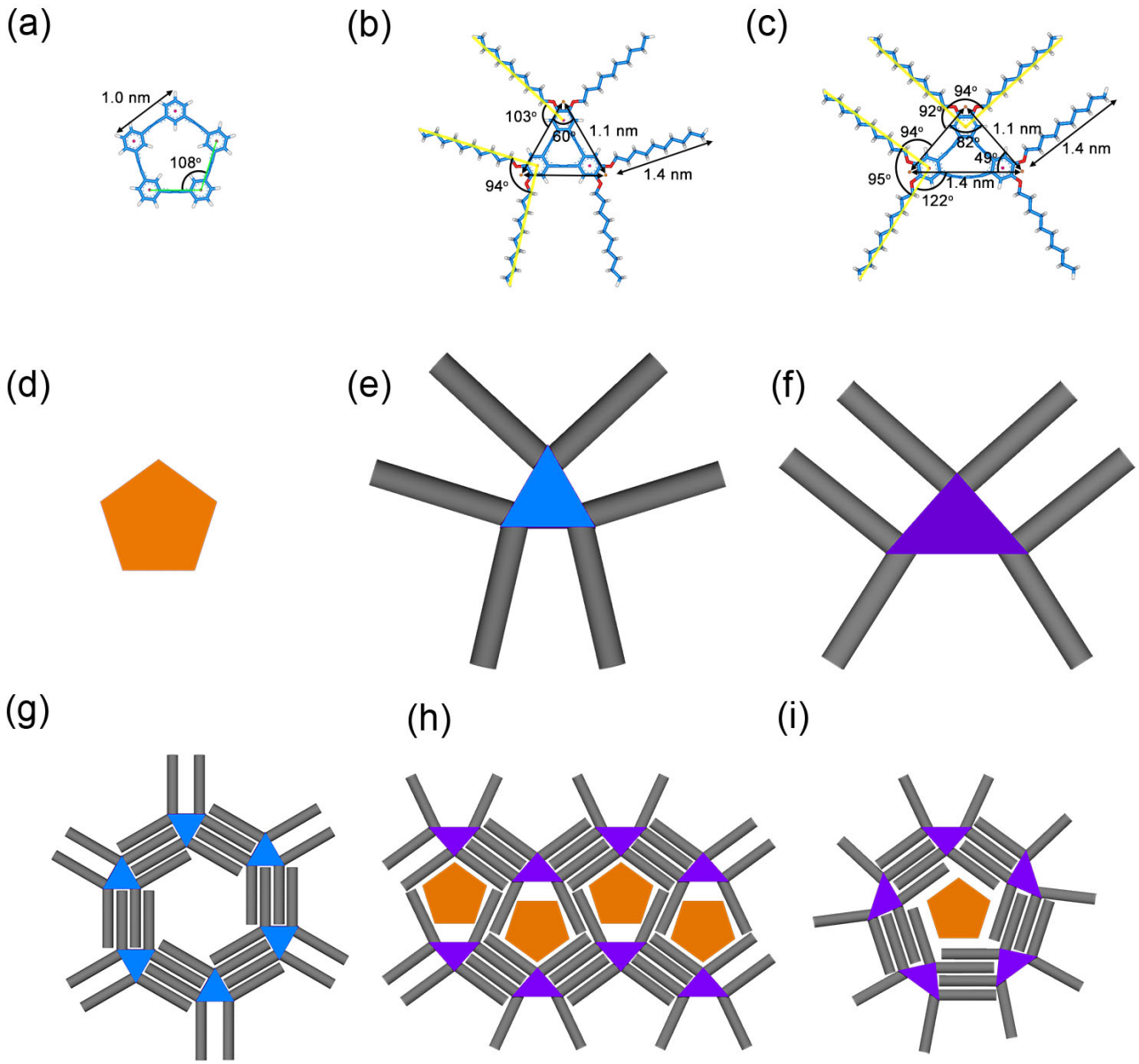

Figure S1. (a, b, c) DFT optimized structures and (d, e, f) schematic representations of **[5]CMPA**, **[12]DBA** and **[14]ISODBA**. **[5]CMPA** is described as a pentagonal tile (d), **[12]DBA** is described as a light blue regular triangle with six grey sticks (e) and **[14]ISODBA** is regarded as a purple isosceles triangle with six grey sticks (f). (g) Schematic model of a honeycomb structure formed by **[12]DBA**. (h, i) Schematic models of conceived linear (d) and cyclic (d) type co-assemblies formed by **[5]CMPA** and **[14]ISODBA**.

3. Domain Size Modulation upon Annealing Treatment

SAMNs of **[14]ISODBA** were investigated at the TCB/graphite interface. **[14]ISODBA** forms three structures at different solute concentrations. The annealing treatment does not lead to structural transformation at the middle concentration, while the coverage of **Phase 1** is increased after annealing treatment at the high concentration (Table S1, Fig. S2).

Table S1. Domain area ratios of **Phases 1-3** in TCB (2.0×10^{-4} M) with or without the annealing treatment.

annealing treatment	concentration (M)	domain area ratio[a]		
		Phase 1	**Phase 2**	**Phase 3**
none	2.0×10^{-4}	30%	32%	37%
80 °C for 3 h		61%	22%	17%

[a]Domain area ratios were determined by 35 large area STM images (80 nm × 80 nm or larger) recorded in three independent experimental sessions (more than 7 images were recorded per session). Domain boundaries and defects of ca. 5–10% of the surface area were excluded from the analysis.

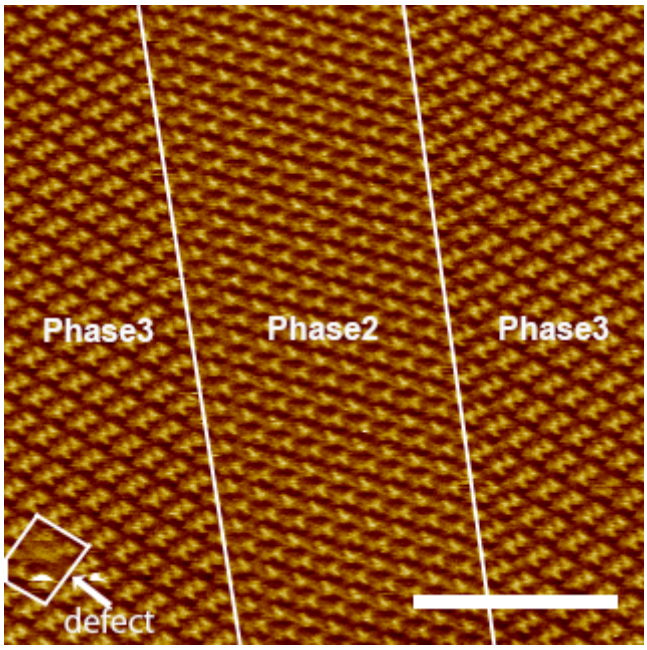

Figure S2. STM image of monolayers formed by **[14]ISODBA** at the TCB/graphite interface (after annealing treatment, concentration; 2.0×10^{-4} M, tunneling parameters; $I_{set} = 120$ pA, $V_{bias} = -0.96$ V). In this image, **Phase 2** and **Phase 3** coexist. White lines and box indicate domain boundaries and defect area, respectively. Scale bar corresponds 10 nm.

4. Additional Information on SAMNs Formation

There is no SAMN formation of **[14]ISODBA** at the lowest solute concentration of 2.0×10^{-6} M in TCB. For concentrations of 2.0×10^{-5} M and higher, **[14]ISODBA** forms SAMNs with distorted hexagonal pores (**Phase 1**, Fig. S3a). In STM images, π-conjugated cores were resolved as bright features because of their higher tunneling efficiency.[6] Therefore, bright triangular features in the STM images correspond to the π-conjugated core of **[14]ISODBA**. Dim lines connecting the triangular π-cores are adsorbed alkyl chains. The four alkyl chains at two short sides of **[14]ISODBA** molecule form [2+2] type alkyl chain interdigitation patterns with adjacent molecules to maximize the intermolecular van der Waals interactions.[3,7] On the other hand, the two alkyl chains at a wide side of the isosceles triangle, one interacts with another molecule to form a [1+1] type intermolecular interaction and the other orients toward a center of the hexagonal pore (Fig. S3a). The alkyl chains are known to be favorably absorbed along with the main symmetric axes of graphite because of epitaxial match.[8] Note that, however, some alkyl chains of **[14]ISODBA** are not parallel to the main symmetric axes of graphite. The angles between the alkyl chain orientations and main symmetric axes of graphite in **Phase 1** are $\alpha = 5 \pm 2°$ and $\beta = 26 \pm 3°$ for the alkyl chains adopting the [2+2] type interdigitation patterns (Table S2). We attribute eight dim spots in the hexagonal pore to co-adsorbed TCB molecules (Fig. S3a).[9,10] Unit cell parameters of **Phase 1** are $a = 4.0 \pm 0.1$ nm, $b = 4.7 \pm 0.1$ nm and $\gamma = 55 \pm 1°$, and the unit cell area is 16 ± 1 nm^2. MM optimized network model is shown in Fig. S3b.

At the highest solute concentration (2.0×10^{-4} M), **[14]ISODBA** forms two different SAMNs, **Phase 2** and **Phase 3**, together with **Phase 1** (Fig. S3c-f and Table S2). In **Phase 2**, **[14]ISODBA** forms a zig-zag molecular row where the π-cores are connected through [2+2] type alkyl chains at both short sides of **[14]ISODBA**. One alkyl chain at the wide side shows a [1+1] type interaction with the adjacent molecule, and another chain orients to the space between the zigzag molecular rows.

In the space between zigzag rows, there are dim spots which are attributed to co-adsorbed TCB molecules (Table S2). The adsorbed alkyl chains forming the [2+2] type interaction pattern are close to parallel to the main symmetric axes of graphite. Unit cell parameters are a = 2.9 ± 0.1 nm, b = 4.8 ± 0.2 nm and γ = 75 ± 2°, and the unit area is 13 ± 1 nm^2. MM optimized network model based on these results is displayed in Fig. S3d.

In the case of **Phase 3**, the molecules form a zigzag molecular row in which each molecule is connected through [2+2] type alkyl chain interdigitation patterns at both short sides of **[14]ISODBA** (Fig. S3e). The other one alkyl chain at the long side is adsorbed along to the zigzag molecular row. Another one was not observed on the surface, and it orients to the solution phase. In the small rectangular pore appears a dim spot which is attributed to a co-adsorbed TCB molecule (Fig. S3e). In this case, all adsorbed alkyl chains are close to parallel to the main symmetric axes of graphite. Unit cell parameters of **Phase 3** are a = 2.5 ± 0.1 nm, b = 3.9 ± 0.1 nm and γ = 89 ± 2°, and the unit area is 10 ± 1 nm^2. MM optimized network model is shown in Fig. S3f.

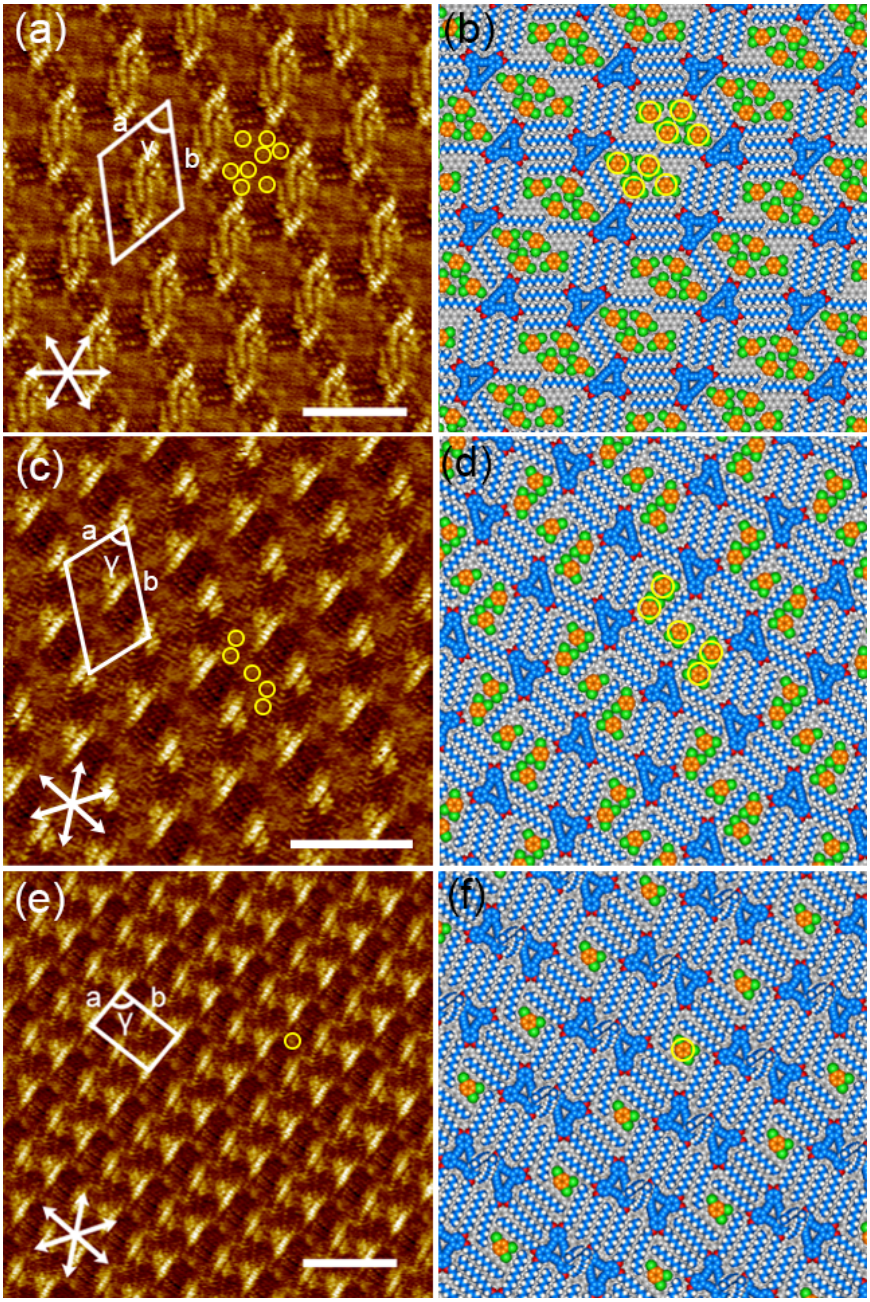

Figure S3. STM images (a, c, e) and molecular models (b, d, f) of **Phase 1**, **Phase 2** and **Phase 3** SAMNs of **[14]ISODBA** at the 1,2,4-trichlorobenzene (TCB)/graphite interface at room temperature (tunneling parameters for (a); I_{set} = 150 pA, V_{bias} = –0.31 V and tunneling parameters for (c, e) are described in Fig. 2). In the images, there are fuzzy bright spots between the molecular rows. Yellow circles in the images (a, c, e) highlight fuzzy bright spots and those in the models (b, d, f) indicate corresponding co-adsorbed TCB molecules, respectively. Scale bars in the STM images are 5 nm.

Table S2. Unit Cell Parameters, Unit Areas and Alkyl Chain Orientations with Respect to the Nearest Main Symmetric Axis of Graphite of Observed SAMNs.[a]

structure	unit cell parameters			area (nm^2)	angles between alkyl chain and main symmetric axes of graphite	
	a (nm)	b (nm)	γ (°)		α (°)	β (°)
Phase 1	4.0 ± 0.1	4.7 ± 0.1	55 ± 1	16 ± 1	5 ± 2	26 ± 3
Phase 2	2.9 ± 0.1	4.8 ± 0.2	75 ± 2	13 ± 1	< 3[b]	< 3[b]
Phase 3	2.5 ± 0.1	3.9 ± 0.1	89 ± 2	10 ± 1	< 3[b]	< 3[b]
Co-crystal	3.4 ± 0.1	4.7 ± 0.1	89 ± 1	16 ± 1	< 3[b]	10 ± 4

[a]When there exist two non-equivalent [2+2] type alkyl chain interdigitation parts in the network, the smaller angles are defined as angles α. These are often imaged as brighter in the image. [b]These are parallel to the main symmetric axes of graphite.

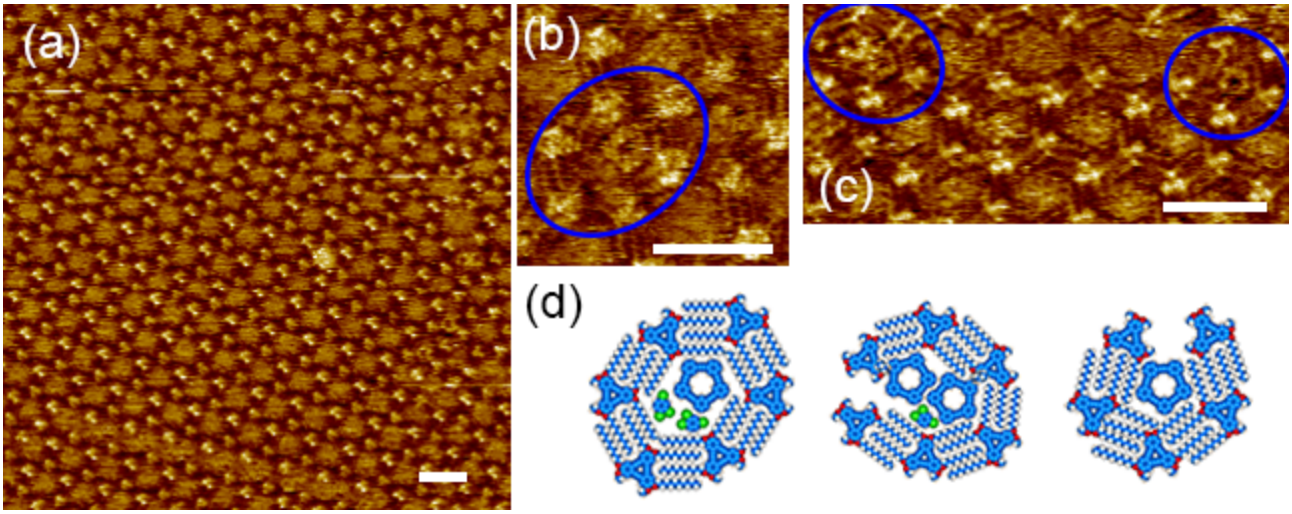

Figure S4. (a-c) STM images of a monolayer formed by a mixture of **[12]DBA** and **[5]CMPA** (no annealing treatment, concentrations; **[12]DBA**: 1.1 × 10^{-5} M, **[5]CMPA**: 4.4 × 10^{-4} M, tunneling parameters; I_{set} = 146 pA, V_{bias} = –0.88 V for (a), I_{set} = 100 pA, V_{bias} = –0.62 V for (b), and I_{set} = 100 pA, V_{bias} = –0.48 V for (c)). Distorted hexagonal pores (defects) with co-adsorbed **[5]CMPA** molecule(s) are highlighted by blue circles in images (b) and (c). (d) Tentative molecular models of the distorted hexagonal pores. In the model, some decyloxy chains orienting to the pore space are substituted with methoxy groups. Scale bars in the images correspond to 5 nm.

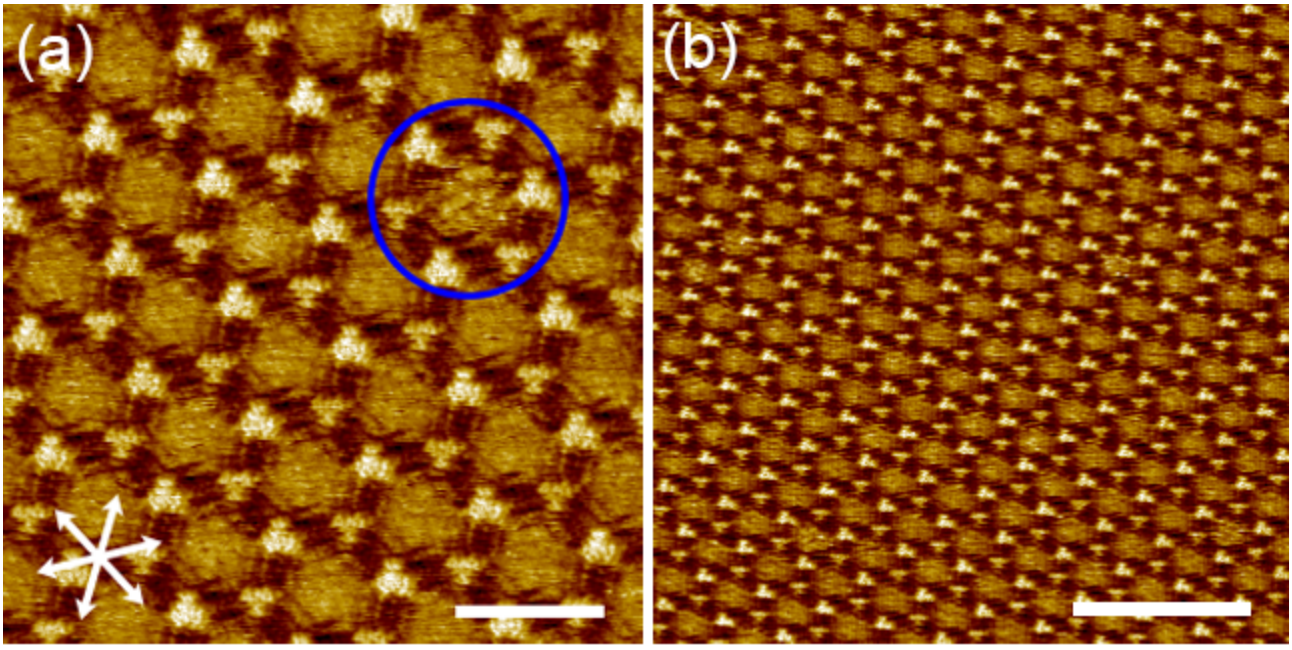

Figure S5. (a) Small area STM image of a honeycomb structure of **[12]DBA** after annealing treatment. Blue circle indicates fuzzy bright feature at the pore. Scale bar corresponds to 5 nm. (b) Large area STM image after annealing treatment. Scale bar in the image corresponds to 10 nm (**[12]DBA**: 1.1×10^{-5} M, **[5]CMPA**: 4.4×10^{-4} M, tunneling parameters for both images; $I_{set} = 100$ pA, $V_{bias} = -0.27$ V).

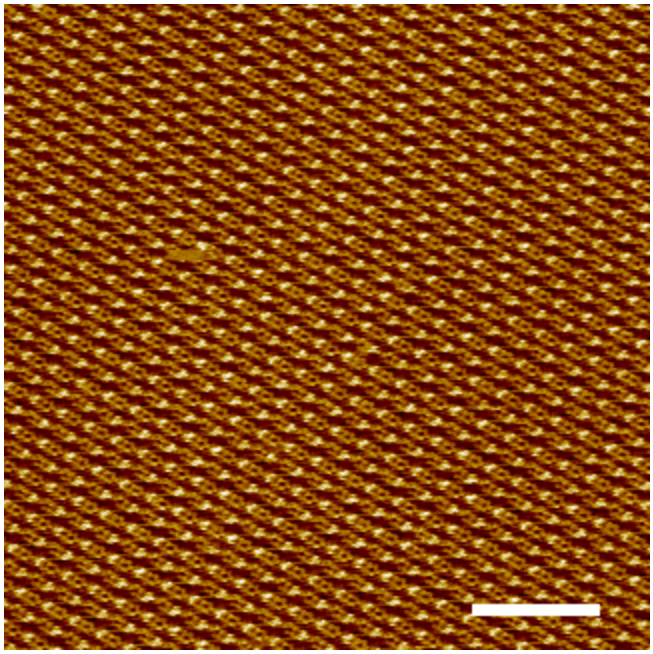

Figure S6. Large area STM image of **Co-crystal**. Scale bar corresponds to 10 nm (after annealing treatment, concentration; **[14]ISODBA**: 1.1×10^{-5} M, **[5]CMPA**: 4.4×10^{-4} M, tunneling parameters; I_{set} = 100 pA, V_{bias} = –0.62 V). The typical domain size after annealing treatment is over 100 nm × 100 nm.

The **Co-crystal** formation was also observed in 1-phenyloctane (Fig. S7), while the observed domain sizes are smaller than those observed in TCB.

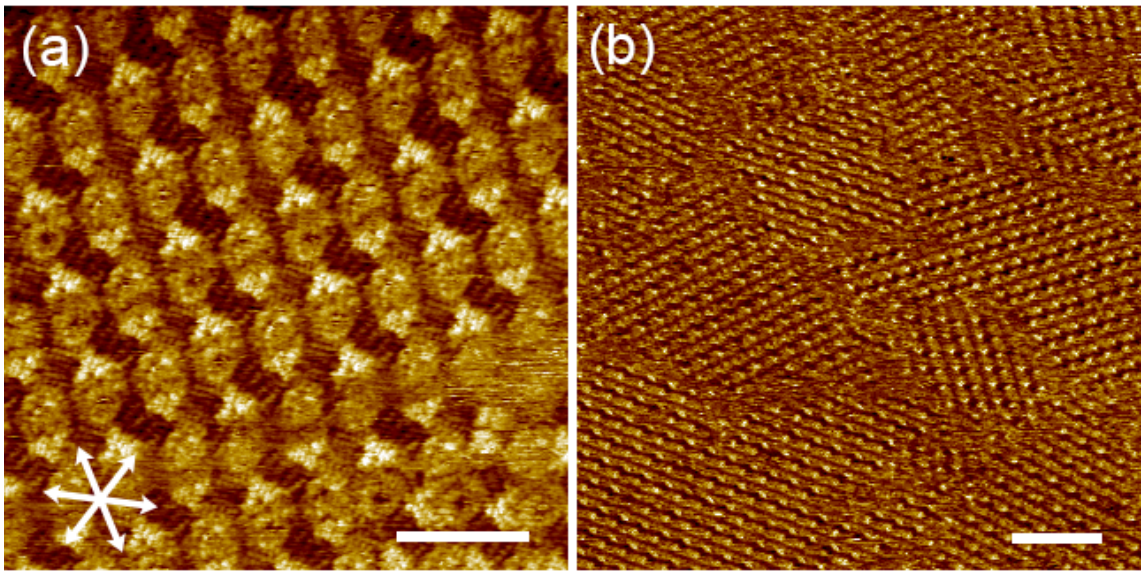

Figure S7. Small (a) and large (b) area STM images of **Co-crystal** formed by a mixture of **[14]DBA** and **[5]CMPA** at the 1-phenyloctane/graphite interface (after annealing treatment, concentration; **[14]DBA**: 1.1×10^{-5} M, **[5]CMPA**: 4.4×10^{-4} M, tunneling parameters; (a) $I_{set} = 100$ pA, $V_{bias} = -0.29$ V, (b) $I_{set} = 100$ pA, $V_{bias} = -0.39$ V). Scale bars in (a) and (b) correspond to 5 and 10 nm, respectively.

5. Energy Estimations for Monolayer Networks by MM Simulations

To estimate the energy changes per single molecule, the results of the MM simulations were analyzed by a procedure which modified the previously reported methods by Gutzler *et al*[11] and by us.[9,12] Table S3 summarizes each energy value.

1. Energy changes upon adsorption of a single **[14]ISODBA** molecule from vacuum to a monolayer without including guest molecules ($\Delta e_{\text{total-single}}$)

·Energy after optimizations of a monolayer network on bi-layered graphite sheets: e_1

·Energy after single point calculations after removal of one **[14]ISODBA** molecule from the optimized network structures of the **[14]ISODBA** molecules on bi-layered graphite sheets: e_2

·Energy of an optimized geometry of a single **[14]ISODBA** molecule under vacuum: e_3

$\Delta e_{\text{total-single}} = e_1 - (e_2 + e_3)$

2. Interaction energy between a **[14]ISODBA** molecule and substrate ($\Delta e_{\text{mol-sub-single}}$) and between **[14]ISODBA** molecules ($\Delta e_{\text{mol-mol-single}}$) upon adsorption of a single **[14]ISODBA** molecule in a monolayer without including guest molecules

·Energy after single point calculations of a single **[14]ISODBA** molecule having identical geometry with that of the optimized monolayer network on the bi-layered graphite sheets: e_4

$\Delta e_{\text{mol-sub-single}} = e_4 - e_3$

$\Delta e_{\text{mol-mol-single}} = (\Delta e_{\text{total-single}} - \Delta e_{\text{mol-sub-single}})$/(number of the **[14]ISODBA** molecules per a unit cell)

3. Enthalpy change upon adsorption of a single **[14]ISODBA** molecule from vacuum to the monolayer network without including guest molecules ($\Delta h_{\text{[14]ISODBA-single}}$)

$\Delta h_{\text{[14]ISODBA-single}} = \Delta e_{\text{mol-mol-single}} + \Delta e_{\text{mol-sub-single}}$

4. Enthalpy changes upon adsorption of guest or solvent molecules from vacuum to a monolayer

network including guest or solvent molecules (Δh_{guest})

·Energy after optimization of a monolayer network including guest or solvent molecules: e_5

·Energy of an optimized geometry of a single guest or solvent molecule under vacuum: e_6

$\Delta h_{guest} = e_5 - ((\text{number of the coadsorbed TCB or } \textbf{[5]CMPA} \text{ molecules per a unit cell}) \times e_6 + e_1)$

5. The energy values ($\Delta e_{mol\text{-}mol\text{-}single}$, $\Delta e_{mol\text{-}sub\text{-}single}$, and $\Delta h_{[14]ISODBA\text{-}single}$) are multiplied by the number of **[14]DBA** molecules per unit cell (2). Then, the calculated energy values and Δh_{guest} value are divided by unit area to afford $\Delta e_{mol\text{-}mol}$, $\Delta e_{mol\text{-}sub}$, $\Delta h_{[14]ISODBA}$ and Δh_{TCB} or $\Delta h_{[5]CMPA}$ as summarized in Table S4. The Δh values are calculated using the following equation.

$\Delta h = \Delta h_{[14]ISODBA} + \Delta h_{TCB}$ or $\Delta h_{[5]CMPA}$

Table S3. Estimated Energies (kcal·mol^{-1}) of **Phases 1-3** and **Co-crystal**.

	Phase 1	**Phase 2**	**Phase 3**	**Co-crystal**
number of **[14]ISODBA** molecules	2	2	2	2
number of TCB or **[5]CMPA** molecules	8	5	1	2
Unit area (nm^2) per PBC	15.6	13.1	9.8	15.6
e_1	–563.4	–567.0	–539.6	–569.4
e_2	–258.3	–260.2	–245.4	–261.7
e_3	–123.8	–123.8	–123.8	–123.8
e_4	–258.3	–260.2	–245.4	–261.7
$\Delta e_{total\text{-}single}$	–181.3	–183.0	–170.4	–183.9
$\Delta e_{mol\text{-}sub\text{-}single}$	–134.4	–136.4	–121.5	–137.8
$\Delta e_{mol\text{-}mol\text{-}single}$	–23.4	–23.3	–24.4	–23.0
$\Delta h_{[14]DBA\text{-}single}$	–157.9	–159.7	–145.9	–160.8
e_5	–745.9	–689.9	–565.8	–810.0
e_6	3.4	3.4	3.4	–30.2
Δh_{guest}	–209.4	–139.7	–29.6	–180.1

Table S4. Calculated Energies and Enthalpies per Unit Area (kcal·mol^{-1}·nm^{-2}) of **Phases 1-3** and **Co-crystal**.

	number of **[14]ISODBA** molecules included per unit cell	number of TCB or **[5]CMPA** molecules included per unit cell	$\Delta e_{\text{mol-sub}}$[a]	$\Delta e_{\text{mol-mol}}$[b]	$\Delta h_{[14]\text{ISODBA}}$[c]	Δh_{TCB} or $\Delta h_{[5]\text{CMPA}}$[d]	Δh[e]
Phase 1	2	8	−17.2	−3.0	−10.1	−13.4	−23.5
Phase 2	2	5	−20.8	−3.6	−12.2	−10.7	−22.9
Phase 3	2	1	−24.8	−5.0	−14.9	−3.0	−17.9
Co-crystal	2	2	−17.7	−2.9	−10.3	−11.5	−21.8

[a]Interaction energies with the substrate upon the adsorption of a single **[14]ISODBA** molecule ($\Delta e_{\text{mol-sub}}$) in each phase. [b]Intermolecular interactions upon adsorption of a single **[14]ISODBA** molecule ($\Delta e_{\text{mol-mol}}$) in each phase. These do not include the interactions between the TCB or **[5]CMPA** and **[14]ISODBA** molecules. [c]Enthalpy change upon adsorption of a single **[14]ISODBA** molecule in each phase ($\Delta e_{\text{mol-sub}} + \Delta e_{\text{mol-mol}}$). [d]Enthalpy change upon co-adsorption of the TCB molecules or **[5]CMPA** in each phase. [e]Total enthalpy change in each phase ($\Delta h_{[14]\text{ISODBA}} + \Delta h_{\text{TCB}}$ or $\Delta h_{[14]\text{ISODBA}} + \Delta h_{[5]\text{CMPA}}$).

6. ^{1}H and ^{13}C NMR Spectra of New Compounds

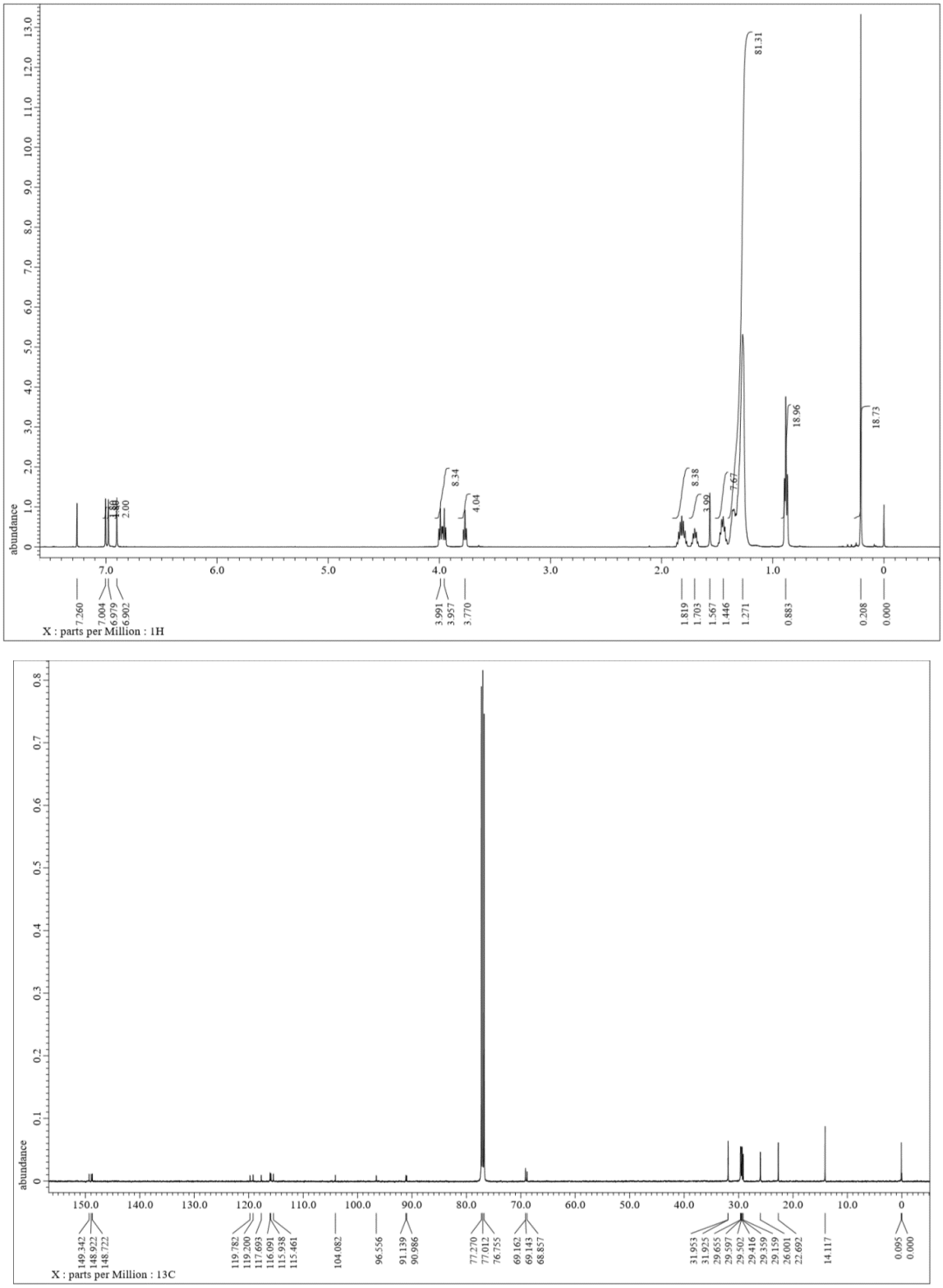

Figure S8. ^{1}H (top) and ^{13}C (bottom) NMR spectra of compound **4**.

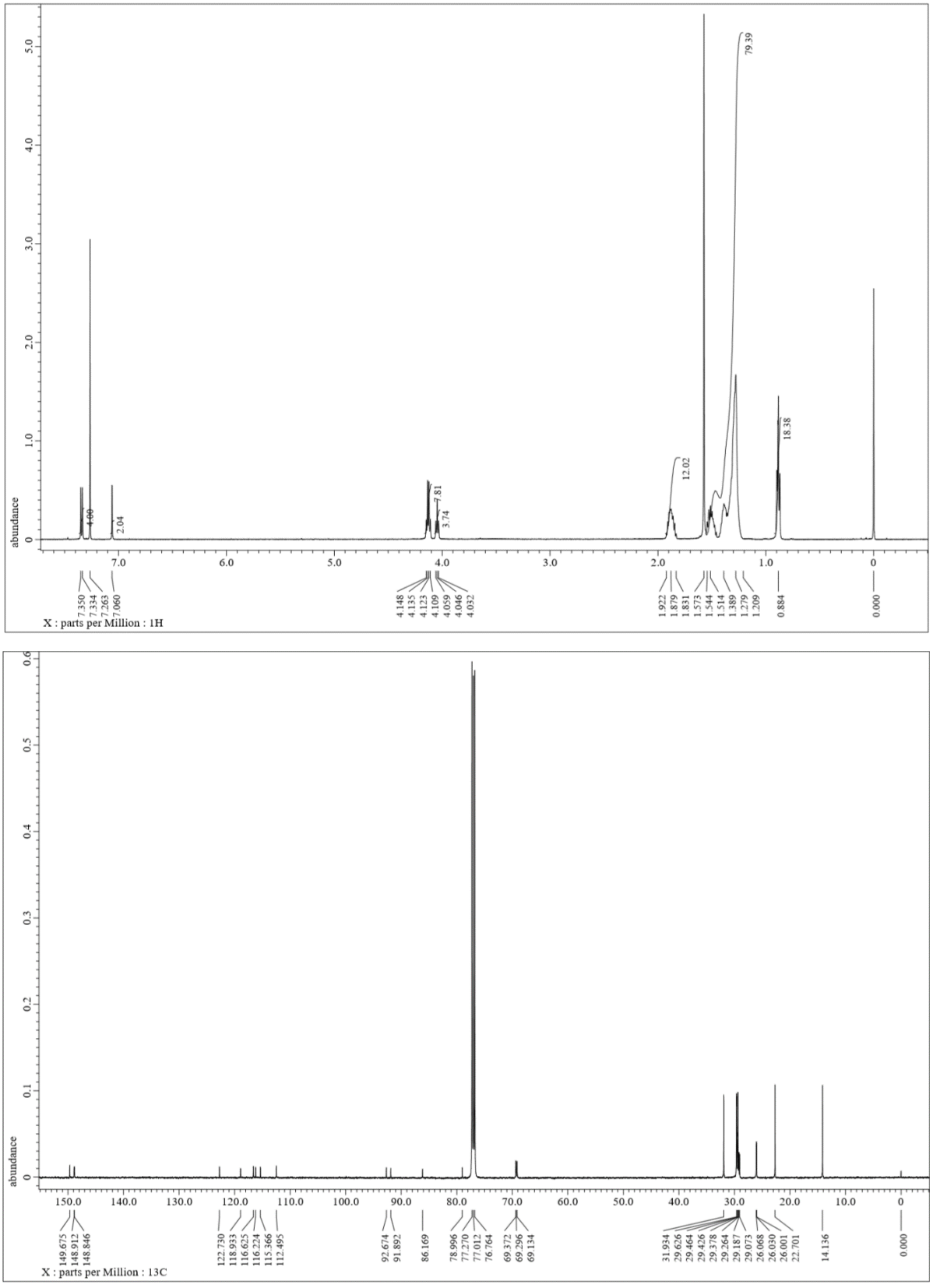

Figure S9. ^{1}H (top) and ^{13}C (bottom) NMR spectra of **[14]ISODBA**.

7. Cartesian Coordinates of Optimized Geometries

C_{2v}-[14]ISODBA

Zero-point correction = 2.019839 (Hartree/Particle)

Thermal correction to Energy = 2.130835

Thermal correction to Enthalpy = 2.131780

Thermal correction to Gibbs Free Energy = 1.831195

Sum of electronic and zero-point Energies = -3805.863220

Sum of electronic and thermal Energies = -3805.752224

Sum of electronic and thermal Enthalpies = -3805.751280

Sum of electronic and thermal Free Energies = -3806.051864

Standard orientation:

Center Number	Atomic Number	Atomic Type	Coordinates (Angstroms) X	Y	Z
1	6	0	0.000000	1.385034	-2.454536
2	6	0	0.000000	0.709415	-1.205956
3	6	0	0.000000	-0.709415	-1.205956
4	6	0	0.000000	-1.385034	-2.454536
5	6	0	0.000000	-0.711631	-3.664169
6	6	0	0.000000	0.711631	-3.664169
7	1	0	0.000000	2.467199	-2.434740
8	1	0	0.000000	-2.467199	-2.434740
9	6	0	0.000000	-1.535752	-0.050380
10	6	0	0.000000	1.535752	-0.050380
11	6	0	0.000000	2.409270	0.802236
12	6	0	0.000000	-2.409270	0.802236
13	6	0	0.000000	3.463392	1.752224

14	6	0	0.000000	3.221390	3.153339
15	6	0	0.000000	4.803735	1.299731
16	6	0	0.000000	4.315155	4.047628
17	6	0	0.000000	5.871987	2.185205
18	1	0	0.000000	4.979659	0.231473
19	6	0	0.000000	5.623575	3.588671
20	1	0	0.000000	4.104545	5.109551
21	6	0	0.000000	-3.463392	1.752224
22	6	0	0.000000	-4.803735	1.299731
23	6	0	0.000000	-3.221390	3.153339
24	6	0	0.000000	-5.871987	2.185205
25	1	0	0.000000	-4.979659	0.231473
26	6	0	0.000000	-4.315155	4.047628
27	6	0	0.000000	-5.623575	3.588671
28	1	0	0.000000	-4.104545	5.109551
29	6	0	0.000000	1.888599	3.612643
30	6	0	0.000000	0.675788	3.770831
31	6	0	0.000000	-1.888599	3.612643
32	6	0	0.000000	-0.675788	3.770831
33	8	0	0.000000	1.297978	-4.890406
34	8	0	0.000000	-1.297978	-4.890406
35	8	0	0.000000	7.183065	1.827849
36	8	0	0.000000	6.730211	4.376987
37	8	0	0.000000	-6.730211	4.376987
38	8	0	0.000000	-7.183065	1.827849
39	6	0	0.000000	-2.722514	-4.966409
40	1	0	-0.888879	-3.123781	-4.457223
41	1	0	0.888879	-3.123781	-4.457223
42	6	0	0.000000	-3.106014	-6.439934
43	1	0	-0.880050	-2.657233	-6.918047
44	1	0	0.880050	-2.657233	-6.918047
45	6	0	0.000000	-4.625156	-6.653259
46	1	0	-0.879129	-5.066019	-6.160315
47	1	0	0.879129	-5.066019	-6.160315
48	6	0	0.000000	-5.022975	-8.135159
49	1	0	-0.878463	-4.581411	-8.628148
50	1	0	0.878463	-4.581411	-8.628148

51	6	0	0.000000	2.722514	-4.966409
52	1	0	-0.888879	3.123781	-4.457223
53	1	0	0.888879	3.123781	-4.457223
54	6	0	0.000000	3.106014	-6.439934
55	1	0	0.880050	2.657233	-6.918047
56	1	0	-0.880050	2.657233	-6.918047
57	6	0	0.000000	4.625156	-6.653259
58	1	0	0.879129	5.066019	-6.160315
59	1	0	-0.879129	5.066019	-6.160315
60	6	0	0.000000	5.022975	-8.135159
61	1	0	0.878463	4.581411	-8.628148
62	1	0	-0.878463	4.581411	-8.628148
63	6	0	0.000000	-7.514794	0.440251
64	1	0	-0.888969	-7.086402	-0.046147
65	1	0	0.888969	-7.086402	-0.046147
66	6	0	0.000000	-9.033288	0.328690
67	1	0	0.880059	-9.422655	0.856247
68	1	0	-0.880059	-9.422655	0.856247
69	6	0	0.000000	-9.516479	-1.127288
70	1	0	0.879124	-9.110934	-1.649669
71	1	0	-0.879124	-9.110934	-1.649669
72	6	0	0.000000	-11.045779	-1.252036
73	1	0	0.878470	-11.451319	-0.729047
74	1	0	-0.878470	-11.451319	-0.729047
75	6	0	0.000000	-6.556898	5.793768
76	1	0	0.888806	-5.985301	6.099412
77	1	0	-0.888806	-5.985301	6.099412
78	6	0	0.000000	-7.939541	6.431157
79	1	0	0.880220	-8.489831	6.074927
80	1	0	-0.880220	-8.489831	6.074927
81	6	0	0.000000	-7.876549	7.963969
82	1	0	0.878911	-7.311875	8.308520
83	1	0	-0.878911	-7.311875	8.308520
84	6	0	0.000000	-9.261585	8.624275
85	1	0	0.878568	-9.826918	8.280352
86	1	0	-0.878568	-9.826918	8.280352
87	6	0	0.000000	6.556898	5.793768

88	1	0	-0.888806	5.985301	6.099412
89	1	0	0.888806	5.985301	6.099412
90	6	0	0.000000	7.939541	6.431157
91	1	0	-0.880220	8.489831	6.074927
92	1	0	0.880220	8.489831	6.074927
93	6	0	0.000000	7.876549	7.963969
94	1	0	-0.878911	7.311875	8.308520
95	1	0	0.878911	7.311875	8.308520
96	6	0	0.000000	9.261585	8.624275
97	1	0	-0.878568	9.826918	8.280352
98	1	0	0.878568	9.826918	8.280352
99	6	0	0.000000	7.514794	0.440251
100	1	0	0.888969	7.086402	-0.046147
101	1	0	-0.888969	7.086402	-0.046147
102	6	0	0.000000	9.033288	0.328690
103	1	0	-0.880059	9.422655	0.856247
104	1	0	0.880059	9.422655	0.856247
105	6	0	0.000000	9.516479	-1.127288
106	1	0	-0.879124	9.110934	-1.649669
107	1	0	0.879124	9.110934	-1.649669
108	6	0	0.000000	11.045779	-1.252036
109	1	0	-0.878470	11.451319	-0.729047
110	1	0	0.878470	11.451319	-0.729047
111	6	0	0.000000	-6.540203	-8.361562
112	1	0	0.878625	-6.981309	-7.867650
113	1	0	-0.878625	-6.981309	-7.867650
114	6	0	0.000000	-6.936717	-9.843628
115	1	0	0.878414	-6.494935	-10.337191
116	1	0	-0.878414	-6.494935	-10.337191
117	6	0	0.000000	-8.453648	-10.073209
118	1	0	0.878500	-8.895494	-9.579636
119	1	0	-0.878500	-8.895494	-9.579636
120	6	0	0.000000	-8.849443	-11.555280
121	1	0	0.878458	-8.408094	-12.049573
122	1	0	-0.878458	-8.408094	-12.049573
123	6	0	0.000000	-11.541062	-2.703904
124	1	0	-0.878619	-11.134408	-3.226548

125	1	0	0.878619	-11.134408	-3.226548
126	6	0	0.000000	-13.070245	-2.827845
127	1	0	0.878419	-13.476476	-2.304653
128	1	0	-0.878419	-13.476476	-2.304653
129	6	0	0.000000	6.540203	-8.361562
130	1	0	-0.878625	6.981309	-7.867650
131	1	0	0.878625	6.981309	-7.867650
132	6	0	0.000000	6.936717	-9.843628
133	1	0	0.878414	6.494935	-10.337191
134	1	0	-0.878414	6.494935	-10.337191
135	6	0	0.000000	8.453648	-10.073209
136	1	0	0.878500	8.895494	-9.579636
137	1	0	-0.878500	8.895494	-9.579636
138	6	0	0.000000	8.849443	-11.555280
139	1	0	0.878458	8.408094	-12.049573
140	1	0	-0.878458	8.408094	-12.049573
141	6	0	0.000000	10.366092	-11.786393
142	1	0	-0.878027	10.807214	-11.293281
143	1	0	0.878027	10.807214	-11.293281
144	6	0	0.000000	10.751964	-13.269116
145	1	0	0.000000	11.840130	-13.400354
146	1	0	0.884617	10.354676	-13.782111
147	1	0	-0.884617	10.354676	-13.782111
148	6	0	0.000000	11.541062	-2.703904
149	1	0	0.878619	11.134408	-3.226548
150	1	0	-0.878619	11.134408	-3.226548
151	6	0	0.000000	13.070245	-2.827845
152	1	0	0.878419	13.476476	-2.304653
153	1	0	-0.878419	13.476476	-2.304653
154	6	0	0.000000	-13.568271	-4.278962
155	1	0	-0.878501	-13.161980	-4.802186
156	1	0	0.878501	-13.161980	-4.802186
157	6	0	0.000000	-15.097311	-4.402456
158	1	0	0.878461	-15.504391	-3.879593
159	1	0	-0.878461	-15.504391	-3.879593
160	6	0	0.000000	13.568271	-4.278962
161	1	0	0.878501	13.161980	-4.802186

162	1	0	-0.878501	13.161980	-4.802186
163	6	0	0.000000	15.097311	-4.402456
164	1	0	0.878461	15.504391	-3.879593
165	1	0	-0.878461	15.504391	-3.879593
166	6	0	0.000000	15.596702	-5.853060
167	1	0	0.878033	15.190715	-6.375468
168	1	0	-0.878033	15.190715	-6.375468
169	6	0	0.000000	-15.596702	-5.853060
170	1	0	-0.878033	-15.190715	-6.375468
171	1	0	0.878033	-15.190715	-6.375468
172	6	0	0.000000	17.124591	-5.966745
173	1	0	0.884613	17.558025	-5.483907
174	1	0	0.000000	17.448839	-7.013736
175	1	0	-0.884613	17.558025	-5.483907
176	6	0	0.000000	-17.124591	-5.966745
177	1	0	0.884613	-17.558025	-5.483907
178	1	0	-0.884613	-17.558025	-5.483907
179	1	0	0.000000	-17.448839	-7.013736
180	6	0	0.000000	-9.205413	10.157256
181	1	0	-0.878503	-8.638451	10.499616
182	1	0	0.878503	-8.638451	10.499616
183	6	0	0.000000	-10.588440	10.821353
184	1	0	-0.878480	-11.155511	10.479111
185	1	0	0.878480	-11.155511	10.479111
186	6	0	0.000000	-10.531197	12.354470
187	1	0	-0.878447	-9.963664	12.696243
188	1	0	0.878447	-9.963664	12.696243
189	6	0	0.000000	-11.912970	13.020767
190	1	0	-0.878489	-12.481271	12.679998
191	1	0	0.878489	-12.481271	12.679998
192	6	0	0.000000	-11.855257	14.553822
193	1	0	-0.878011	-11.288033	14.894423
194	1	0	0.878011	-11.288033	14.894423
195	6	0	0.000000	-13.239040	15.211500
196	1	0	0.000000	-13.163379	16.304945
197	1	0	-0.884626	-13.817593	14.917750
198	1	0	0.884626	-13.817593	14.917750

199	6	0	0.000000	9.205413	10.157256
200	1	0	0.878503	8.638451	10.499616
201	1	0	-0.878503	8.638451	10.499616
202	6	0	0.000000	10.588440	10.821353
203	1	0	0.878480	11.155511	10.479111
204	1	0	-0.878480	11.155511	10.479111
205	6	0	0.000000	10.531197	12.354470
206	1	0	0.878447	9.963664	12.696243
207	1	0	-0.878447	9.963664	12.696243
208	6	0	0.000000	11.912970	13.020767
209	1	0	-0.878489	12.481271	12.679998
210	1	0	0.878489	12.481271	12.679998
211	6	0	0.000000	11.855257	14.553822
212	1	0	0.878011	11.288033	14.894423
213	1	0	-0.878011	11.288033	14.894423
214	6	0	0.000000	13.239040	15.211500
215	1	0	-0.884626	13.817593	14.917750
216	1	0	0.000000	13.163379	16.304945
217	1	0	0.884626	13.817593	14.917750
218	6	0	0.000000	-10.366092	-11.786393
219	1	0	0.878027	-10.807214	-11.293281
220	1	0	-0.878027	-10.807214	-11.293281
221	6	0	0.000000	-10.751964	-13.269116
222	1	0	0.000000	-11.840130	-13.400354
223	1	0	-0.884617	-10.354676	-13.782111
224	1	0	0.884617	-10.354676	-13.782111

***D*$_{5h}$-[5]CMPA**

Zero-point correction= 0.453895 (Hartree/Particle)

Thermal correction to Energy= 0.485508

Thermal correction to Enthalpy= 0.486452

Thermal correction to Gibbs Free Energy= 0.390424

Sum of electronic and zero-point Energies= -1535.605937

Sum of electronic and thermal Energies= -1535.574324

Sum of electronic and thermal Enthalpies= -1535.573379

Sum of electronic and thermal Free Energies= -1535.669408

Standard orientation:

Center Number	Atomic Number	Atomic Type	Coordinates (Angstroms) X	Y	Z
1	6	0	1.223600	5.137610	0.000000
2	6	0	0.000000	4.447210	0.000000
3	6	0	-1.223600	5.137610	0.000000
4	6	0	-1.212300	6.546410	0.000000
5	6	0	0.000000	7.234010	0.000000
6	6	0	1.212300	6.546410	0.000000
7	1	0	0.000000	3.362910	0.000000
8	1	0	-2.153500	7.086910	0.000000
9	1	0	0.000000	8.320410	0.000000
10	1	0	2.153500	7.086910	0.000000
11	6	0	2.436400	4.387810	0.000000
12	6	0	-2.436400	4.387810	0.000000
13	6	0	-3.420166	3.673062	0.000000
14	6	0	3.420166	3.673062	0.000000
15	6	0	4.508044	2.751321	0.000000

16	6	0	4.229548	1.374263	0.000000
17	6	0	5.851384	3.175918	0.000000
18	6	0	5.264270	0.423896	0.000000
19	1	0	3.198317	1.039196	0.000000
20	6	0	6.879952	2.235432	0.000000
21	1	0	6.074583	4.238076	0.000000
22	6	0	6.600627	0.869986	0.000000
23	1	0	7.913180	2.571148	0.000000
24	1	0	7.405520	0.141875	0.000000
25	6	0	-4.508044	2.751321	0.000000
26	6	0	-4.229548	1.374263	0.000000
27	6	0	-5.851384	3.175918	0.000000
28	6	0	-5.264270	0.423896	0.000000
29	1	0	-3.198317	1.039196	0.000000
30	6	0	-6.879952	2.235432	0.000000
31	1	0	-6.074583	4.238076	0.000000
32	6	0	-6.600627	0.869986	0.000000
33	1	0	-7.913180	2.571148	0.000000
34	1	0	-7.405520	0.141875	0.000000
35	6	0	-4.925944	-0.961246	0.000000
36	6	0	-4.550179	-2.117733	0.000000
37	6	0	4.925944	-0.961246	0.000000
38	6	0	4.550179	-2.117733	0.000000
39	6	0	4.009724	-3.437199	0.000000
40	6	0	2.614004	-3.597868	0.000000
41	6	0	4.828654	-4.583585	0.000000
42	6	0	2.029898	-4.875628	0.000000
43	1	0	1.976669	-2.720651	0.000000
44	6	0	4.252044	-5.852437	0.000000
45	1	0	5.907799	-4.467635	0.000000
46	6	0	2.867112	-6.008729	0.000000
47	1	0	4.890614	-6.731353	0.000000
48	1	0	2.423363	-6.999226	0.000000
49	6	0	-4.009724	-3.437199	0.000000
50	6	0	-2.614004	-3.597868	0.000000
51	6	0	-4.828654	-4.583585	0.000000
52	6	0	-2.029898	-4.875628	0.000000

53	1	0	-1.976669	-2.720651	0.000000
54	6	0	-4.252044	-5.852437	0.000000
55	1	0	-5.907799	-4.467635	0.000000
56	6	0	-2.867112	-6.008729	0.000000
57	1	0	-4.890614	-6.731353	0.000000
58	1	0	-2.423363	-6.999226	0.000000
59	6	0	0.608001	-4.981893	0.000000
60	6	0	-0.608001	-4.981893	0.000000

***D*$_{3h}$-[5]CMPA**

Zero-point correction= 2.009103 (Hartree/Particle)

Thermal correction to Energy= 2.118377

Thermal correction to Enthalpy= 2.119321

Thermal correction to Gibbs Free Energy= 1.822407

Sum of electronic and zero-point Energies= -3729.720534

Sum of electronic and thermal Energies= -3729.611260

Sum of electronic and thermal Enthalpies= -3729.610315

Sum of electronic and thermal Free Energies= -3729.907230

Standard orientation:

Center Number	Atomic Number	Atomic Type	Coordinates (Angstroms) X	Y	Z
1	6	0	2.029812	1.990163	0.000000
2	6	0	2.756520	3.199497	0.000000
3	6	0	4.146238	3.214269	0.000000
4	6	0	4.856757	1.983613	-0.000000
5	6	0	4.149106	0.787467	-0.000000
6	6	0	2.738438	0.762787	-0.000000
7	1	0	2.199622	4.128021	0.000000
8	1	0	4.674782	-0.159082	-0.000000
9	6	0	0.608308	2.014549	0.000000
10	6	0	-0.608308	2.014549	-0.000000
11	6	0	2.048805	-0.480464	-0.000000
12	6	0	1.440497	-1.534085	0.000000
13	6	0	-2.029812	1.990163	-0.000000
14	6	0	-2.756520	3.199497	-0.000000
15	6	0	-2.738438	0.762787	0.000000
16	6	0	-4.146238	3.214269	-0.000000
17	1	0	-2.199622	4.128021	-0.000000
18	6	0	-4.149106	0.787467	0.000000

19	6	0	-4.856757	1.983613	0.000000
20	1	0	-4.674782	-0.159082	0.000000
21	6	0	0.708626	-2.752950	0.000000
22	6	0	1.392586	-3.986965	0.000000
23	6	0	-0.708626	-2.752950	0.000000
24	6	0	0.710519	-5.197882	0.000000
25	1	0	2.475160	-3.968939	0.000000
26	6	0	-1.392586	-3.986965	0.000000
27	6	0	-0.710519	-5.197882	0.000000
28	1	0	-2.475160	-3.968939	0.000000
29	6	0	-2.048805	-0.480464	0.000000
30	6	0	-1.440497	-1.534085	0.000000
31	8	0	4.916319	4.335394	0.000000
32	8	0	6.212720	2.089960	-0.000000
33	8	0	1.296402	-6.425354	0.000000
34	8	0	-1.296402	-6.425354	0.000000
35	8	0	-4.916319	4.335394	-0.000000
36	8	0	-6.212720	2.089960	0.000000
37	6	0	6.992229	0.895537	0.000000
38	1	0	6.753552	0.292615	0.888830
39	1	0	6.753552	0.292615	-0.888830
40	6	0	8.459502	1.302531	0.000000
41	1	0	8.647999	1.930658	0.880024
42	1	0	8.647999	1.930658	-0.880024
43	6	0	9.405988	0.095292	0.000000
44	1	0	9.200654	-0.533410	-0.879056
45	1	0	9.200654	-0.533410	0.879056
46	6	0	10.887506	0.494510	0.000000
47	1	0	11.092510	1.123827	0.878459
48	1	0	11.092510	1.123827	-0.878459
49	6	0	11.844530	-0.704389	0.000000
50	1	0	11.638555	-1.333767	-0.878601
51	1	0	11.638555	-1.333767	0.878601
52	6	0	13.325498	-0.303804	0.000000
53	1	0	13.530803	0.325997	0.878414
54	1	0	13.530803	0.325997	-0.878414
55	6	0	14.285249	-1.500750	0.000000

56	1	0	14.080016	-2.130607	-0.878499
57	1	0	14.080016	-2.130607	0.878499
58	6	0	15.765829	-1.099424	0.000000
59	1	0	15.971920	-0.469618	0.878460
60	1	0	15.971920	-0.469618	-0.878460
61	6	0	16.726839	-2.295300	0.000000
62	1	0	16.521682	-2.924312	-0.878029
63	1	0	16.521682	-2.924312	0.878029
64	6	0	18.202994	-1.885011	0.000000
65	1	0	18.447339	-1.283920	0.884615
66	1	0	18.862610	-2.760371	0.000000
67	1	0	18.447339	-1.283920	-0.884615
68	6	0	4.271672	5.607679	0.000000
69	1	0	3.630188	5.702440	-0.888830
70	1	0	3.630188	5.702440	0.888830
71	6	0	5.357776	6.674878	0.000000
72	1	0	5.995998	6.524058	0.880024
73	1	0	5.995998	6.524058	-0.880024
74	6	0	4.785519	8.098178	0.000000
75	1	0	4.138380	8.234705	0.879056
76	1	0	4.138380	8.234705	-0.879056
77	6	0	5.872011	9.181602	0.000000
78	1	0	6.519517	9.044482	0.878459
79	1	0	6.519517	9.044482	-0.878459
80	6	0	5.312246	10.609858	0.000000
81	1	0	4.664202	10.746167	-0.878601
82	1	0	4.664202	10.746167	0.878601
83	6	0	6.399646	11.692122	0.000000
84	1	0	7.047724	11.555020	0.878414
85	1	0	7.047724	11.555020	-0.878414
86	6	0	5.842937	13.121763	0.000000
87	1	0	5.194848	13.258955	-0.878499
88	1	0	5.194848	13.258955	0.878499
89	6	0	6.930786	14.203321	0.000000
90	1	0	7.579259	14.066898	0.878460
91	1	0	7.579259	14.066898	-0.878460
92	6	0	6.375631	15.633517	0.000000

93	1	0	5.728313	15.770353	-0.878029
94	1	0	5.728313	15.770353	0.878029
95	6	0	7.469029	16.706761	0.000000
96	1	0	7.040754	17.715685	0.000000
97	1	0	8.111762	16.617825	0.884615
98	1	0	8.111762	16.617825	-0.884615
99	6	0	-4.271672	5.607679	0.000000
100	1	0	-3.630188	5.702440	0.888830
101	1	0	-3.630188	5.702440	-0.888830
102	6	0	-5.357776	6.674878	0.000000
103	1	0	-5.995998	6.524058	0.880024
104	1	0	-5.995998	6.524058	-0.880024
105	6	0	-4.785519	8.098178	0.000000
106	1	0	-4.138380	8.234705	0.879056
107	1	0	-4.138380	8.234705	-0.879056
108	6	0	-6.992229	0.895537	-0.000000
109	1	0	-6.753552	0.292615	-0.888830
110	1	0	-6.753552	0.292615	0.888830
111	6	0	-5.872011	9.181602	0.000000
112	1	0	-6.519517	9.044482	0.878459
113	1	0	-6.519517	9.044482	-0.878459
114	6	0	-8.459502	1.302531	-0.000000
115	1	0	-8.647999	1.930658	0.880024
116	1	0	-8.647999	1.930658	-0.880024
117	6	0	-5.312246	10.609858	0.000000
118	1	0	-4.664202	10.746167	0.878601
119	1	0	-4.664202	10.746167	-0.878601
120	6	0	-9.405988	0.095292	-0.000000
121	1	0	-9.200654	-0.533410	-0.879056
122	1	0	-9.200654	-0.533410	0.879056
123	6	0	-6.399646	11.692122	0.000000
124	1	0	-7.047724	11.555020	0.878414
125	1	0	-7.047724	11.555020	-0.878414
126	6	0	-10.887506	0.494510	-0.000000
127	1	0	-11.092510	1.123827	0.878459
128	1	0	-11.092510	1.123827	-0.878459
129	6	0	-11.844530	-0.704389	-0.000000

130	1	0	-11.638555	-1.333767	-0.878601
131	1	0	-11.638555	-1.333767	0.878601
132	6	0	-5.842937	13.121763	0.000000
133	1	0	-5.194848	13.258955	0.878499
134	1	0	-5.194848	13.258955	-0.878499
135	6	0	-13.325498	-0.303804	-0.000000
136	1	0	-13.530803	0.325997	0.878414
137	1	0	-13.530803	0.325997	-0.878414
138	6	0	-6.930786	14.203321	0.000000
139	1	0	-7.579259	14.066898	0.878460
140	1	0	-7.579259	14.066898	-0.878460
141	6	0	-6.375631	15.633517	0.000000
142	1	0	-5.728313	15.770353	0.878029
143	1	0	-5.728313	15.770353	-0.878029
144	6	0	-7.469029	16.706761	0.000000
145	1	0	-8.111762	16.617825	0.884615
146	1	0	-7.040754	17.715685	0.000000
147	1	0	-8.111762	16.617825	-0.884615
148	6	0	-14.285249	-1.500750	-0.000000
149	1	0	-14.080016	-2.130607	-0.878499
150	1	0	-14.080016	-2.130607	0.878499
151	6	0	-15.765829	-1.099424	-0.000000
152	1	0	-15.971920	-0.469618	0.878460
153	1	0	-15.971920	-0.469618	-0.878460
154	6	0	-16.726839	-2.295300	-0.000000
155	1	0	-16.521682	-2.924312	-0.878029
156	1	0	-16.521682	-2.924312	0.878029
157	6	0	-18.202994	-1.885011	-0.000000
158	1	0	-18.862610	-2.760371	-0.000000
159	1	0	-18.447339	-1.283920	0.884615
160	1	0	-18.447339	-1.283920	-0.884615
161	6	0	-2.720557	-6.503216	0.000000
162	1	0	-3.123364	-5.995055	0.888830
163	1	0	-3.123364	-5.995055	-0.888830
164	6	0	2.720557	-6.503216	0.000000
165	1	0	3.123364	-5.995055	-0.888830
166	1	0	3.123364	-5.995055	0.888830

167	6	0	-3.101726	-7.977409	0.000000
168	1	0	-2.652001	-8.454716	0.880024
169	1	0	-2.652001	-8.454716	-0.880024
170	6	0	3.101726	-7.977409	0.000000
171	1	0	2.652001	-8.454716	-0.880024
172	1	0	2.652001	-8.454716	0.880024
173	6	0	-4.620469	-8.193470	0.000000
174	1	0	-5.062274	-7.701295	0.879056
175	1	0	-5.062274	-7.701295	-0.879056
176	6	0	4.620469	-8.193470	0.000000
177	1	0	5.062274	-7.701295	-0.879056
178	1	0	5.062274	-7.701295	0.879056
179	6	0	-5.015495	-9.676112	0.000000
180	1	0	-4.572993	-10.168309	0.878459
181	1	0	-4.572993	-10.168309	-0.878459
182	6	0	-6.532284	-9.905469	0.000000
183	1	0	-6.974353	-9.412401	0.878601
184	1	0	-6.974353	-9.412401	-0.878601
185	6	0	-6.925851	-11.388317	0.000000
186	1	0	-6.483079	-11.881018	0.878414
187	1	0	-6.483079	-11.881018	-0.878414
188	6	0	5.015495	-9.676112	0.000000
189	1	0	4.572993	-10.168309	-0.878459
190	1	0	4.572993	-10.168309	0.878459
191	6	0	-8.442312	-11.621013	0.000000
192	1	0	-8.885167	-11.128348	0.878499
193	1	0	-8.885167	-11.128348	-0.878499
194	6	0	6.532284	-9.905469	0.000000
195	1	0	6.974353	-9.412401	-0.878601
196	1	0	6.974353	-9.412401	0.878601
197	6	0	6.925851	-11.388317	0.000000
198	1	0	6.483079	-11.881018	-0.878414
199	1	0	6.483079	-11.881018	0.878414
200	6	0	-8.835043	-13.103897	0.000000
201	1	0	-8.392661	-13.597280	0.878460
202	1	0	-8.392661	-13.597280	-0.878460
203	6	0	8.442312	-11.621013	0.000000

204	1	0	8.885167	-11.128348	-0.878499
205	1	0	8.885167	-11.128348	0.878499
206	6	0	-10.351207	-13.338217	0.000000
207	1	0	-10.793370	-12.846041	0.878029
208	1	0	-10.793370	-12.846041	-0.878029
209	6	0	8.835043	-13.103897	0.000000
210	1	0	8.392661	-13.597280	-0.878460
211	1	0	8.392661	-13.597280	0.878460
212	6	0	10.351207	-13.338217	0.000000
213	1	0	10.793370	-12.846041	-0.878029
214	1	0	10.793370	-12.846041	0.878029
215	6	0	-10.733965	-14.821750	0.000000
216	1	0	-10.335577	-15.333904	0.884615
217	1	0	-11.821857	-14.955314	0.000000
218	1	0	-10.335577	-15.333904	-0.884615
219	6	0	10.733965	-14.821750	0.000000
220	1	0	10.335577	-15.333904	-0.884615
221	1	0	11.821857	-14.955314	0.000000
222	1	0	10.335577	-15.333904	0.884615

---

8. References

1. N. Miyaura and A. Suzuki, *Org. Synth.*, 1990, **68**, 130.

2. D. R. Coulson, L. C. Satek and S. O. Grim, *Inorg. Synth.*, 1972, **13**, 121.

3. K. Tahara, S. Furukawa, H. Uji-i, T. Uchino, T. Ichikawa, J. Zhang, and W. Mamdouh, M. Sonoda, F. C. De Schryver, S. De Feyter and Y. Tobe, *J. Am. Chem. Soc.*, 2006, **128**, 16613.

4. Q. Zhou, P. J. Carroll and T. M. Swager, *J. Org. Chem.*, 1994, **59**, 1294.

5. M. J. Frisch, G. W. Trucks, H. B. Schlegel, G. E. Scuseria, M. A. Robb, J. R. Cheeseman, G. Scalmani, V. Barone, G. A. Petersson, H. Nakatsuji, X. Li, M. Caricato, A. V. Marenich, J. Bloino, B. G. Janesko, R. Gomperts, B. Mennucci, H. P. Hratchian, J. V. Ortiz, A. F. Izmaylov, J. L. Sonnenberg, D. Williams-Young, F. Ding, F. Lipparini, F. Egidi, J. Goings, B. Peng, A. Petrone, T. Henderson, D. Ranasinghe, V. G. Zakrzewski, J. Gao, N. Rega, G. Zheng, W. Liang, M. Hada, M. Ehara, K. Toyota, R. Fukuda, J. Hasegawa, M. Ishida, T. Nakajima, Y. Honda, O. Kitao, H. Nakai, T. Vreven, K. Throssell, J. A., Jr. Montgomery, J. E. Peralta, F. Ogliaro, M. J. Bearpark, J. J. Heyd, E. N. Brothers, K. N. Kudin, V. N. Staroverov, T. A. Keith, R. Kobayashi, J. Normand, K. Raghavachari, A. P. Rendell, J. C. Burant, S. S. Iyengar, J. Tomasi, M. Cossi, J. M. Millam, M. Klene, C. Adamo, R. Cammi, J. W. Ochterski, R. L. Martin, K. Morokuma, O. Farkas, J. B. Foresman and D. J. Fox, *Gaussian 16*, Revision A.03, Gaussian, Inc., Wallingford CT, 2016.

6. R. Lazzaroni, A. Calderone, G. Lambin, J. P. Rabe and J. L. Brédas, *Synth. Met.*, 1991, **41**, 525.

7. K. Tahara, C. A. Johnson, T. Fujita, M. Sonoda, F. C. De Schryver, S. De Feyter, M. M. Haley and Y. Tobe, *Langmuir*, 2007, **20**, 10190.

8. A. J. Groszek, *Proc. R. Soc. London Ser. A*, 1970, **314**, 473.

9. K. Tahara, R. Nakayama, M. Maeda, S. De Feyter and Y. Tobe, *J. Phys. Chem. C*, 2019, **123**, 27020.

10. T. J. Keller, J. Bahr, K. Gratzfeld, N. Schönfelder, M. A. Majewski, M. Stępień, S. Höger and S.-S. Jester, *Beilstein J. Org. Chem.*, 2019, **15**, 1848.

11. R. Gutzler, T. Sirtl, J. F. Dienstmaier, K. Mahata, W. M. Heckl, M. Schmittel and M. Lackinger, *J. Am. Chem. Soc.*, 2010, **132**, 5084.

12. M. O. Blunt, J. Adisoejoso, K. Tahara, K. Katayama, M. Van der Auweraer, Y. Tobe and S. De Feyter, *J. Am. Chem. Soc.*, 2013, **135**, 12068.